NANO LETTERS

2002
Vol. 2, No. 11
1287−1291

Hierarchical ZnO Nanostructures

Jing Yu Lao, Jian Guo Wen, and Zhi Feng Ren*

Department of Physics, Boston College, Chestnut Hill, Massachusetts 02467

Received August 15, 2002; Revised Manuscript Received August 30, 2002

ABSTRACT

A variety of novel hierarchical nanostructures with 6-, 4-, and 2-fold symmetries have been successfully grown by a vapor transport and condensation technique. It was found that the major core nanowires are single-crystal In_2O_3 with 6, 4, and 2 facets, and the secondary nanorods are single-crystal hexagonal ZnO and grow either perpendicular on or slanted to all the facets of the core In_2O_3 nanowires. The core In_2O_3 nanowires have diameters of about 50–500 nm, whereas the secondary ZnO nanorods have diameters of about 20–200 nm. Depending on the diameter of the core In_2O_3 nanowires, the secondary ZnO nanorods grow either as a single row or multiple rows. These hierarchical heteronanostructures may find applications in a variety of fields such as field emission, photovoltaics, transparent EMI shielding, supercapacitors, fuel cells, high strength and multifunctional nanocomposites, etc. that require not only high surface area but also structural integrity.

ZnO is a very interesting material for its potential applications in numerous fields. In the form of thin films, ZnO is a very promising alternative in flat display screens[1−3] for tin-doped indium oxides (ITO), of which there is a limited natural source. ZnO is a potential sensor of NH_3[4] and a photocatalyst to reduce the emission of NO_x.[5,6] ZnO has also been demonstrated to be efficient light-emitting diodes and laser diodes in the UV/visible range.[7−9] With the successful synthesis of p-type ZnO thin films,[10] p−n homojunctions have been realized.[11] Recently, ZnO[12−14] and In_2O_3[12,15] nanowires and nanoribbons have been synthesized, which may find applications in nanoelectronics, such as ultraviolet lasing which has been observed at room temperature from aligned straight ZnO nanowires.[16] Here we report that many novel hierarchical ZnO nanostructures are grown from In_2O_3 nanowires by a thermal vapor transport and condensation technique.[17] These nanostructures have basic 6-, 4-, and 2-fold structural symmetries. This preparation method opens a brand new field for synthesizing the similar hierarchical heteronanostructures of other complex systems.

Hierarchical ZnO nanostructures have been synthesized on In_2O_3 core nanowires by a vapor transport and condensation process.[17] ZnO, In_2O_3, and graphite powders were mixed thoroughly and then placed at the sealed end of a one-end sealed quartz tube. A graphite foil was used as the collector at the open end of the quartz tube to collect the nanostructures (Si, $LaAlO_3$, etc. have also been used to collect the deposits). The whole assembly was finally pushed into a ceramic tube of a tube furnace pumped by a rotary pump. The vacuum in the ceramic tube was kept at around 0.5 to 2.5 Torr. The mixed powders were heated to between 950 and 1000 °C and held for 30 min. The temperature at where the nanostructures were grown was controlled to be about 820−870 °C due to the temperature gradient in the ceramic tube.

Figure 1 shows the typical scanning electron microscopy (SEM) images of the ZnO nanostructures at low and medium magnifications, respectively. The low magnification image in Figure 1a shows the large quantity of such nanostructures. The medium magnification in Figure 1b clearly shows that there are three major structural symmetries, i.e., 6-, 4-, and 2-fold, as marked. However, closer examination of these nanostructures reveals that there are a few subsymmetries associated with each major symmetry. For 6-fold, we have identified three subsymmetries as 6S-, 6M-, and 6M*-fold (see the definition of the symmetry symbols in reference 18). For 4-fold, we have identified five subsymmetries as 4S-, 4S*[1]-, 4S*[2]-, 4M-, and 4M*-fold.[18] For 2-fold symmetry, we have identified three subsymmetries as 2S-, 2S*-, and 2M-fold.[18] The details of all the nanostructures with 2-fold symmetries are still under investigation due to their different growth mechanism that is probably similar to ZnO−SnO_2 system.[19] In general, the length of the major In_2O_3 core nanowires along the axis can be as long as tens of micrometers as shown in Figure 1a and the diameter is about 50−500 nm, whereas the length of the secondary ZnO nanorods grown on the major In_2O_3 core nanowires ranges from 0.2 to a few micrometers, with diameters ranging from 20 to 200 nm. Powder X-ray diffraction (XRD) measurements show that the samples are mixtures of hexagonal ZnO (wurtzite) and cubic In_2O_3. From the XRD spectra, lattice constants for ZnO are derived as $a = 3.249$ Å and $c = 5.206$ Å, consistent with the standard values for bulk ZnO,[20] whereas the lattice constant for the cubic In_2O_3 is $a = 10.118$ Å, which is in good agreement with the reported bulk value.[20]

During SEM examination, we often observed areas with a certain symmetry as the majority. In Figure 2 we present

* Corresponding author. E-mail: renzh@bc.edu.

10.1021/nl025753t CCC: $22.00
Published on Web 09/13/2002

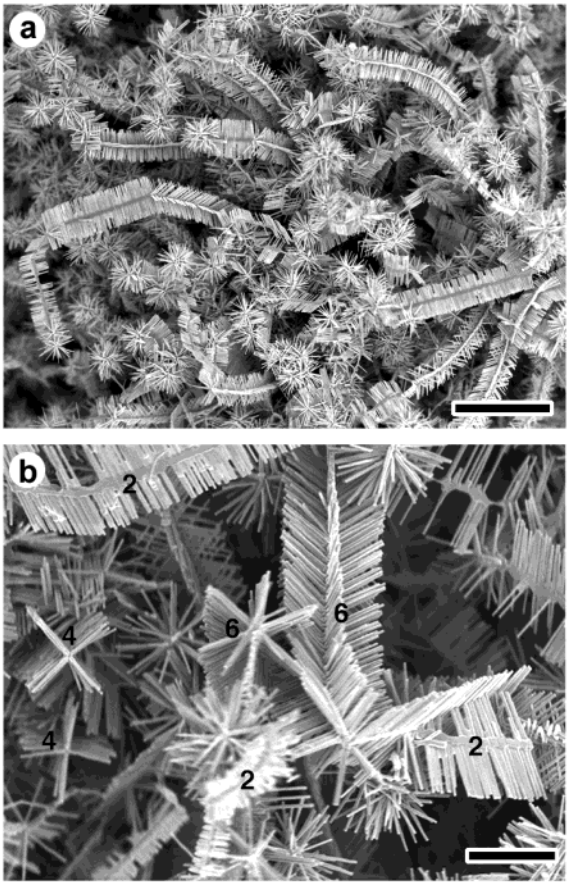

Figure 1. SEM images of the ZnO nanostructures synthesized by the vapor transport and condensation technique. (a) Low magnification SEM image of the ZnO nanostructures to show the abundance. Scale bar, 10 μm. (b) Medium magnification SEM image of ZnO nanostructures to show the various structural symmetries. Three major basic symmetries of 6-, 4-, 2-fold were clearly seen. Scale bar, 3 μm.

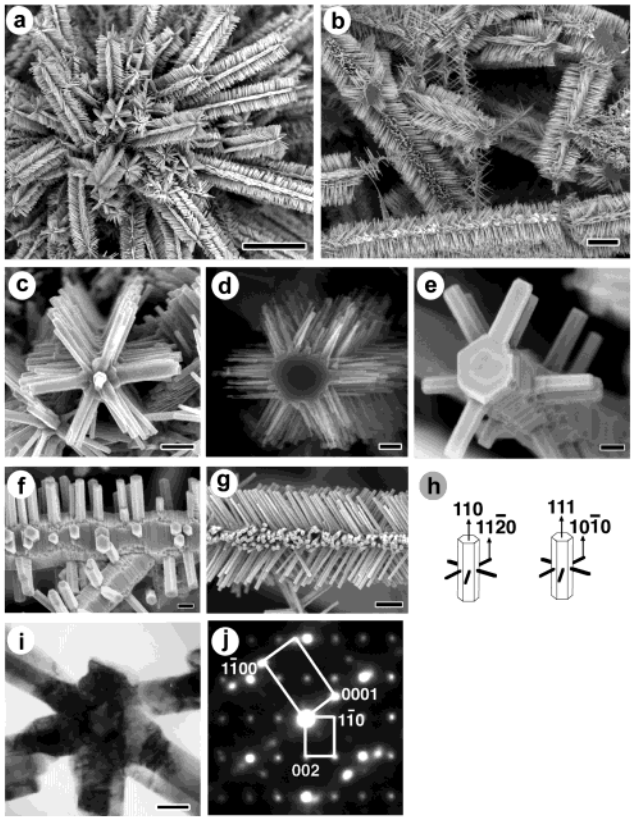

Figure 2. SEM and TEM images, selected area diffraction patterns, and the schematic growth models of the 6-fold ZnO nanostructures. (a) SEM image showing the abundance of the 6S-fold symmetry. Scale bar, 10 μm. (b) SEM image showing the 6M-fold symmetry. (c) High magnification SEM image of the 6S-fold symmetry. (d) High magnification SEM image of the 6M-fold symmetry. (e) Head-on look at a 6S-fold symmetry to show the hexagonal nature of the major core nanowire. (f) Side view of the structure in (e) to show the hexagonal nature of all the secondary ZnO nanorods and their same growth orientations with the major In_2O_3 core nanowire. (g) 6M*-fold symmetry, where the nanorods are not perpendicular to the major core. (h) Schematic diagram of orientation relationships between the major In_2O_3 core nanowire and the secondary ZnO nanorods with the core along the [110] direction (h left) and along [111] direction (h right). (i) Cross-sectional bright-field TEM image of 6-fold symmetry to show the six facets of the central core. (j) Selected-area electron diffraction pattern of (i) corresponding to the major In_2O_3 core and the secondary ZnO nanorods. Scale bar, (b), (c), (g), 1 μm; (d−f), (i), 200 nm.

SEM and transmission electron microscopy (TEM) images[21] in medium and high magnifications to show the 6-fold nanostructures in detail. Figure 2a is a medium magnification of the area with the basic 6S-fold nanostructure as the majority, and Figure 2b is the 6M-fold symmetry. Obviously, when the major core nanowire is small, the secondary nanorods grow in a single row as shown in Figure 2a and Figure 2c. When the major core nanowire is large enough, multiple rows of secondary nanorods form on the major nanowire, as shown in Figure 2b and Figure 2d. The reason they grow into 6-fold symmetry is because of the hexagonal symmetry of the major core as clearly shown in Figure 2e and Figure 2f. It is clearly shown that not only the major core is hexagonal but also the secondary nanorods are hexagonal and aligned in the same direction with each other as shown in Figure 2f. Figure 2g is the SEM image of 6M*-fold, where the nanorods are not perpendicular to the major core. The transmission electron microscopy (TEM) contrast image shown in Figure 2i clearly indicates the hexagonal nature of the In_2O_3 nanocore (lighter contrast in the center).[21] Energy-dispersive X-ray spectroscopy (EDS) composition analysis shows that all the secondary nanorods are pure ZnO and the major core nanowire is In_2O_3. Structural studies by electron diffraction indicate that the major core nanowire is cubic In_2O_3 with lattice parameter of $a = 10.1$ Å (the reason the cubic In_2O_3 grows into hexagonal nanowires is explained later). Selected-area electron diffraction patterns shown in Figure 2j point out that the major cores are along the [110] or [001] zone axes of In_2O_3. All of the secondary nanorods grow along the [0001] direction of ZnO.

In certain areas, we also observed the 4-fold nanostructures as the majority, as shown in Figure 3. Figure 3a is the medium magnification SEM image showing the abundance of 4-fold nanostructures. Under closer examination of high magnification, we found at least five variations for the 4-fold symmetry. Figure 3b is the high magnification SEM image of the basic 4S-fold to show the single row of the secondary ZnO nanorods perpendicular to the major In_2O_3 core nano-

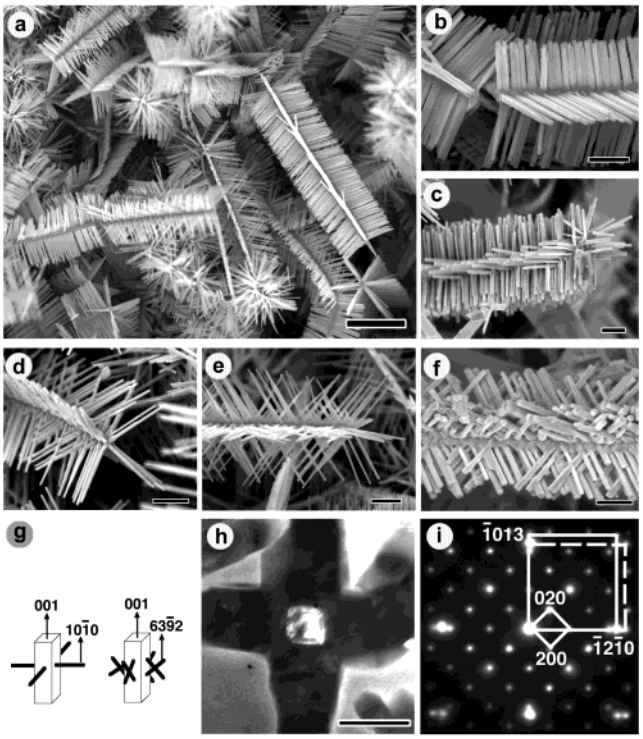

Figure 3. SEM and TEM images, selected area diffraction patterns, and the schematic growth models of the 4-fold ZnO nanostructures. (a) Medium magnification SEM image showing the abundance of the 4-fold nanostructures. Scale bar, 5 μm. (b) High magnification SEM image showing the 4S-fold symmetry. (c) High magnification SEM image showing the 4M-fold symmetry. (d) High magnification SEM image of the 4S*[1]-fold symmetry. (e) High magnification SEM image of the 4S*[2]-fold symmetry. (f) High magnification SEM image of the 4M*-fold symmetry. (g) Schematic model of the 4S- and 4S*-fold symmetry. (h) Cross-sectional bright-field TEM image of 4-fold symmetry to show the four facets of the central core. (i) Selected-area electron diffraction pattern of (h) corresponding to the major In_2O_3 core and the secondary ZnO nanorods. The diffraction consists of two sets of patterns; the small rectangle corresponds to the [00$\bar{1}$] zone axis of In_2O_3 while the large solid one corresponds to [63$\bar{9}$2] zone axis of ZnO. The dashed rectangle is from another arm perpendicular to the solid rectangle. Scale bars are 1 μm for (b−e), and 500 nm for (f), 200 nm for (h).

wire. Similar to what was observed in the 6-fold nanostructures, when the major In_2O_3 core nanowire is large enough, we also observed multiple rows of ZnO nanorods perpendicular to the major In_2O_3 core nanowire. This subsymmetry is identified as 4M-fold as shown in Figure 3c. In addition, we have also observed that the secondary ZnO nanorods are not always perpendicular to the major In_2O_3 core nanowire but grow at certain angles with the In_2O_3 core nanowire. Again, when the major In_2O_3 core nanowire is small, the secondary ZnO nanorods grow in a single row as shown in Figure 3d and Figure 3e. In Figure 3e, the same angle exists in all four directions, whereas in Figure 3d it only exists in the two opposite directions (parallel to the page), and the other two opposite directions are perpendicular to the major In_2O_3 core nanowire (into and out-of the page). We define these two nanostructures as 4S*[1]- and 4S*[2]-fold, respectively. Certainly, when the major In_2O_3 core nanowire is large enough, multiple rows of ZnO nanorods grow with an angle in all four directions as shown in Figure 3f. It is defined as

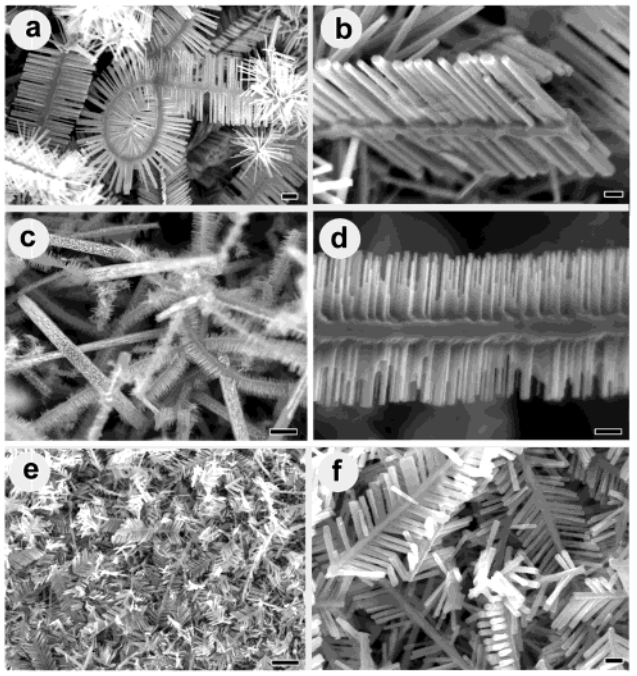

Figure 4. SEM images of the 2-fold nanostructures. (a) Medium SEM image to show the abundance of the 2S-fold symmetry. (b) High magnification of 2S-fold symmetry. (c) Low magnification SEM image to show the abundance of the 2M-fold symmetry. (d) High magnification SEM image of 2M-fold symmetry. (e) Low magnification SEM image to show the abundance of the 2S*-fold symmetry. (f) High magnification SEM image of 2S*-fold symmetry. The scale bars are 1 μm for (a), (c), (e) and 200 nm for (b), (d), (f).

4M*-fold symmetry. Figure 3g is the growth model. Figure 3h and Figure 3i are the TEM bright field image and selected area diffraction patterns, respectively, which are discussed in detail later.

In addition to the 6- and 4-fold symmetrical nanostructures, we have also observed the basic 2-fold nanostructures as shown in Figure 4. But due to the different growth mechanism from 6- and 4-fold, the detailed structural symmetry and growth mechanism studies are still under investigation and will be reported in the future.[19] Here we present only the SEM images to show that such structures were obtained successfully. Figure 4a is a medium magnification SEM image to show the abundance of the basic 2S-fold symmetry, meaning that the secondary ZnO nanorods are perpendicular to the major core nanowire as clearly shown in the high magnification SEM image in Figure 4b. Its variations have been observed and identified so far as 2S*- and 2M-fold. Figure 4c and Figure 4d show the SEM images in low and high magnifications of the 2M-fold symmetry, respectively. Figure 4e and Figure 4f are the low and high magnification SEM images to show the abundance and close look-up of the 2S*-fold, respectively.

It is believed that there are more variations of the 6-, 4-, and 2-fold symmetries. With further research, the missing symmetries of the 6-, 4-, and 2-fold could be found in these ZnO nanostructures also.

Orientation relationships between the major In_2O_3 core nanowire and the secondary ZnO nanorods are obtained from

Table 1. Observed Orientation Relationships between the Major In_2O_3 Core Nanowire and the Secondary ZnO Nanorods

core axis	orientation relationship
$[110]_{In2O3}$ (Figure 2h)	$[110]_{In2O3}//[11\bar{2}0]_{ZnO}$
	$[222]_{In2O3}//[0001]_{ZnO}$
$[111]_{In2O3}$ (Figure 2h)	$[111]_{In2O3}//[10\bar{1}0]_{ZnO}$
	$[11\bar{2}]_{In2O3}//[1\bar{2}10]_{ZnO}$
	$[1\bar{1}0]_{In2O3} \perp [0001]_{ZnO}$
$[001]_{In2O3}$ (Figure 3g)	$[001]_{In2O3}//[10\bar{1}0]_{ZnO}$
	$[100]_{In2O3}//[\bar{1}2\bar{1}0]_{ZnO}$
	$[001]_{In2O3} \perp [0001]_{ZnO}$
$[001]_{In2O3}$ (Figure 3g)	$[001]_{In2O3}//[63\bar{9}2]_{ZnO}$
	$[110]_{In2O3}//[\bar{1}2\bar{1}0]_{ZnO}$
	$[\bar{1}10]_{In2O3}//[\bar{1}013]_{ZnO}$

selected-area diffraction patterns shown in Figure 2j for the 6-fold symmetry and Figure 3i for the 4-fold symmetry. In each diffraction pattern, one can see two sets of diffraction spots, one from the major In_2O_3 core nanowire and the other from the secondary ZnO nanorods. The diffraction pattern in Figure 2j can be indexed using the [110] zone axis of In_2O_3 and the $[11\bar{2}0]$ zone axis of ZnO. So, the crystallographic relationship is $[110]_{In2O3}//[11\bar{2}0]_{ZnO}$ for the 6-fold symmetry. In Figure 3i, the diffraction pattern can be indexed using the [001] zone axis of In_2O_3 and the $[63\bar{9}2]$ zone axis of ZnO. So, the [001] zone axis of In_2O_3 nanowire is parallel to the $[63\bar{9}2]$ zone axis of the ZnO nanorods.

When the In_2O_3 nanowire is along the [001] direction, the core nanowire is enclosed by $\pm(100)$ and $\pm(010)$ facets (Figure 3i). ZnO nanorods grow on each facet of the In_2O_3 nanowire according to the orientation relationships as listed in Table 1. There are two major orientation relationships, corresponding to the observed 4- and 4*-fold symmetries, respectively. The orientation relationship in the 4-fold symmetry is $[001]_{In2O3}//[10\bar{1}0]_{ZnO}$, $[100]_{In2O3}//[\bar{1}2\bar{1}0]_{ZnO}$. In this case, $[001]_{In2O3} \perp [0001]_{ZnO}$, which means all ZnO nanorods in the four arms grow perpendicular to the core nanowire as shown in Figure 3b, because ZnO nanorods grow along the [0001] direction. In the case of 4*-fold symmetry, $[001]_{In2O3}//[63\bar{9}2]_{ZnO}$, so the angle between ZnO nanorod and core nanowire is equal to the angle between $[63\bar{9}2]_{ZnO}$, and $[0001]_{ZnO}$, which is around 60°. This is why a tilted 4*-fold symmetry is often observed in SEM images. Because there is no difference between $\pm [63\bar{9}2]_{ZnO}$, for the growth of a nanorod on a [001] core In_2O_3 nanowire, nanorods can grow with an angle of either 60 or 120 degrees, which resulted in all the variations of the tilted growth as shown in Figure 3d and Figure 3e.

When In_2O_3 is along the [110] directions, the core nanowire is enclosed by $\pm(1\bar{1}2)$, $\pm(1\bar{1}\bar{2})$, and $\pm(1\bar{1}0)$ facets. The angle between each of these adjacent facets is very close to 60°, so a quasi 6-fold symmetry is often observed when an In_2O_3 nanowire grows along the [110] direction. In addition to the [001] and [110] directions, In_2O_3 nanowires are also found to grow along the [111] direction, as shown in Figure 2e and Figure 2f. Hexagon end planes at the ends of the core nanowire (Figure 2e) can be clearly identified in the SEM images, providing strong evidence that the core nanowire grows along the [111] zone axis of In_2O_3. When this type of nanostructure lies in the observation plane, we can also clearly observe hexagon end planes at the end of nanorods (Figure 2f). It indicates that the nanorods grow along the [0001] zone axis of ZnO. The orientation relationship determined by the facets appearing in Figure 2e and Figure 2f is also listed in Table 1. In conclusion, several orientation relationships between ZnO nanorods and In_2O_3 nanowires have been found. The orientation relationships, as schematically shown in Figure 2h and Figure 3g and as listed in Table 1 can be understood using the theory of the near coincidence site lattice. For example, the In_2O_3 *a* plane is 4-fold symmetry with $a = 10.18$ Å and the ZnO *c* plane is 6-fold symmetry with $a = 3.24$ Å, which results in a lattice mismatch of about 3.7% (a factor of 3 for the In_2O_3 *a* axis to the ZnO *a* axis), a reasonable value for epitaxial growth.

The heteroepitaxial nature of ZnO nanorods from In_2O_3 cores gives many possible crystal orientation relations between the cores and nanorods, thus resulting in so many different ZnO nanorod orientations with respect to the core. Therefore, the symmetry of these hierarchical nanostructures is dependent on the crystallographic orientation of the In_2O_3 core nanowires. The orientation of the In_2O_3 nanowire along the [110] or [111] direction creates all of the 6-fold symmetries, whereas along the [001] direction produced all the 4-fold symmetries. Because no catalyst is used in the system, the In_2O_3 nanowire growth should be based on the vapor−solid mechanism.[22] On the other hand, it is more difficult to define the ZnO nanorod growth mechanism. Probably ZnO nanorods also grow based on the vapor−solid mechanism[22] because the In_2O_3 core is covered by a ZnO layer that can be the base for further ZnO nanorod growth. Compared to the aligned ZnO grown by the vapor−liquid−solid mechanism[16] with source temperature around 900 °C, the metal and/or metal oxide vapor pressure here is much higher. This high vapor pressure is necessary for the growth of the hierarchical structures. The growth conditions such as temperature, pressure, and source component ratios are correlated to affect the supersaturation rate and the structure formed.

It is not completely clear what exactly happened between the In_2O_3 and ZnO during the growth that so many complicated structures formed. In the ZnO−In_2O_3−graphite powder system, it is possible that InO_x vaporizes first and condenses on the collector due to the temperature gradient and oxygen partial pressure, and forms into either hexagonal or tetragonal or rectangular In_2O_3 nanowires. Then, ZnO_x vaporizes later and grows on the facets of the existing In_2O_3 nanowires so that 6-, 4-, and 2-fold symmetries are formed. Naturally, cubic In_2O_3 prefers to grow along [001] direction to form the 4-fold symmetry, instead of the [110] or [111] direction to form the 6-fold symmetry. A simple concerted growth mechanism that the inner In_2O_3 nanowire and the external ZnO structure may develop nearly at the same time, and then random fluctuations in the early stages of the nucleation might direct the growth in one direction instead of another cannot be true simply due to the fact that isolated In_2O_3 nanowires with ZnO nanorods just starting have been observed in many samples.

In summary, the work is far from complete in the aspects of synthesizing all of the possible symmetrical nanostructures of ZnO, the microstructure studies, and the growth mechanism; however, we feel that the various nanostructures of ZnO reported here will have numerous potential applications in a variety of fields such as field emission, photovoltaics, transparent EMI shielding, supercapacitors, fuel cells, high strength and multifunctional nanocomposites, etc. In general, with certain modification, the method reported in this article to synthesize such hierarchical nanostructures is applicable to many other oxides, carbides, nitrides, etc. To fabricate nanostructures in a controlled way is a challenge for the development of nanoscience and nanotechnology. We showed that a heteroepitaxial growth of nanorods on a nanowire could be realized in the ZnO−In_2O_3 system. This opens a brand new field to not only nanomaterials synthesis but also their applications in numerous fields.

Acknowledgment. The authors thank M. Dresselhaus at MIT for reading the manuscript and D. Wang and W. Li for the helpful discussion. This work is supported partly by The U.S. Army Natick Soldier Systems Center under grants DAAD16-00-C-9227 and DAAD16-02-C-0037, partly by the DOE under a grant DE-FG02-00ER45805, and partly by the NSF under a grant ECS-0103012.

References

(1) Ginley, D. S.; Bright, C. *Mater. Res. Bull.* **2000**, *25*, 15−18.
(2) Lewis, B. G.; Paine, D. C. *Mater. Res. Bull.* **2000**, *25*, 22−27.
(3) Freeman, A. J.; Poeppelmeier, K. R.; Mason, T. O.; Chang, R. P. H.; Marks, T. J. *Mater. Res. Bull.* **2000**, *25*, 45−51.
(4) Sberveglieri, G.; Groppelli, S.; Nelli, P.; Tintinelli, A.; Giunta, G. *Sens. Actuators, B* **1995**, *25*, 588−590.
(5) Rodriguez, J. A.; Jirsak, T.; Dvorak, J.; Sambasivan, S.; Fischer, D. *J. Phys. Chem. B* **2000**, *104*, 319−328.
(6) Yumoto, H.; Inoue, T.; Li, S. J.; Sako, T.; Nishiyama, K. *Thin Solid Films* **1999**, *345*, 38−41.
(7) Ohta, H. et al. *Appl. Phys. Lett.* **2000**, *77*, 475−477.
(8) Aoki, T.; Hatanaka, Y.; Look, D. C. *Appl. Phys. Lett.* **2000**, *76*, 3257−3258.
(9) Yokogawa, T. et al. *Jpn. J. Appl. Phys. Part 2-Lett* **1996**, *35*, L314-L316.
(10) Minegishi, K. et al. *Jpn. J. Appl. Phys. Part 2-Lett* **1997**, *36*, L1453-L1445.
(11) Xiong, G. et al. *Appl. Phys. Lett.* **2002**, *80*, 1195−1197.
(12) Pan, Z. W.; Dai, Z. R.; Wang, Z. L. *Science* **2001**, *291*, 1947−1949.
(13) Li, Y.; Meng, G. W.; Zhang, L. D.; Phillipp, F. *Appl. Phys. Lett.* **2000**, *76*, 2011−2013.
(14) Li, J. Y.; Chen, X. L.; Li, H.; He, M.; Qiao, Z. Y. *J. Cryst. Growth* **2001**, *233*, 5−7.
(15) Zheng, M. J.; Zhang, L. D.; Li, G. H.; Zhang, X. Y.; Wang, X. F. *Appl. Phys. Lett.* **2001**, *79*, 839−841.
(16) Huang, M. H. et al. *Science* **2001**, *292*, 1897−1899.
(17) Lao, J. Y.; Wen, J. G.; Wang, D. Z.; Ren, Z. F. *Int. J. Nanosci.*, in press.
(18) Definition of the symmetry symbols: for example, in 4S*[1]-, the first character, such as 6 or 4 or 2, means the basic 6-, 4-, and 2-fold symmetry of the major core nanowires, respectively. The second character S or M indicates the single or multiple rows of the secondary ZnO nanorods. If there is nothing after S or M, all of the ZnO nanorods are perpendicular to the major In_2O_3 core nanowire. The third symbol * means that the secondary nanorods are having an angle with the major core nanowire. The number 1 or 2 after the symbol * means that not all the secondary ZnO nanorods branches have an angle with the core nanowire.
(19) Wen, J. G.; Lao, J. Y.; Wang, D. Z.; Ren, Z. F., in preparation.
(20) Powder Diffraction File Release 2000, PDF Maintenance 6.0 (International Center for Diffraction Data, Pennsylvania).
(21) The TEM specimen were prepared as follows. As-synthesized nanomaterials were scratched off the graphite foil onto a holey carbon TEM specimen grid, then a drop of acetone was applied to disperse the nanomaterials so that individual nanostructures can be easily examined. Because of the projection nature of TEM image and multiple arms of the nanorods, TEM images of these nanomaterials are always complex to study. Furthermore, clear diffraction contrast images of the cores cannot be obtained in such a configuration due to their large thickness along the electron beam direction. Cross-sectional TEM along the core nanowire direction was introduced to observe the core structure and the orientation relationship between the arms and the core. Samples for cross-sectional TEM were prepared as follows. Given the brittle nature of the nanomaterials, we penetrated the films with M-Bond 610 epoxy resin (M-Line Accessories, Raleigh, NC) to provide mechanical stiffness. M-Bond 610 epoxy has very low viscosity and curing is time and temperature dependent. The viscosity of the epoxy is very low, so it easily impregnates pores and structure of nanomaterials can be preserved. The sample was cured at a temperature of 120 °C for 2 h. The hardened thin foils containing graphite substrate were then cut, glued together following the standard cross-sectional TEM sample preparation technique. Mechanical thinning by a tripod polisher and ion milling (low angle, voltage, and current) was done to thin the sample to electron transparency. Before TEM observation, a low voltage and gun current were used to polish both sides for 10 min.
(22) Levitt, A. P., Ed.; Whisker Technology; Wiley-Interscience: New York, 1970.

NL025753T